Supplementary Information (SI) for Nanoscale

This Journal is © The Royal Society Chemistry 2025

Rational design of self-assembled monolayer composition for efficient perovskite/Si tandem solar cells

Min Sup Kim,[a‡] So Jeong Park,[a‡] Geon Pyo Hong,[a] Jin Young Kim*[abc]

[a.] Department of Materials Science and Engineering, Seoul National University, Seoul 08826, Republic of Korea

[b.] Research Institute of Advanced Materials (RIAM), Seoul National University, Seoul 08826, Republic of Korea

[c.] School of Transdisciplinary Innovations, Seoul National University, Seoul 08826, Republic of Korea

*Corresponding Authors: Jin Young Kim; **Email**: jykim.mse@snu.ac.kr

‡ These authors contribute equally to this work.

Experimental Section

Materials and methods

Materials

Indium tin oxide (ITO) substrates (20.5 mm x 20.5 mm) were purchased from AMG-Tech. Formamidinium iodide (FAI), ammonium thiocyanate (NH_4SCN) and propane-1,3-diammonium iodide ($PDAI_2$) were purchased from Greatcell Solar. Lead iodide (PbI_2) was purchased from Alfa Aesar. Cesium iodide (CsI), lead bromide ($PbBr_2$), lead chloride ($PbCl_2$), polyethylenimine ethoxylated (PEIE), methylamine solution (33 wt.% ethanol), ethanol, dimethylformamide (DMF), toluene, 2-propanol (IPA), chlorobenzene (CB) and methanol were purchased from Sigma-Aldrich. [4-(3,6-Dimethoxy-9H-carbazol-9-yl)butyl]phosphonic acid (MeO-4PACz) and 4-(3,6-Dibromo-9H-carbazol-9-yl)butyl)phosphonic acid (Br-4PACz) were purchased from TCI chemicals. C_{60} was purchased from Nano-C.

Perovskite film fabrication

ITO-coated glass substrates were sequentially cleaned by sonication in detergent, deionized water, and isopropanol, followed by UV–ozone treatment for 15 min.

MeO-4PACz and Br-4PACz were individually dissolved in ethanol at a concentration of 0.3 mg mL^{-1}, and subsequently mixed at various weight ratios of Br-4PACz to MeO-4PACz (1:4, 4:1, and 8:1) to form mixed self-assembled monolayer (SAM) solutions. The SAM solution was spin-coated at 3000 rpm onto the cleaned ITO substrate and annealed at 100 °C for 10 min to form the hole transport layer (HTL).

The perovskite precursor solution (1.5 M) was prepared by dissolving FAI, CsI, MABr, PbI_2, and $PbBr_2$ in a mixed solvent of DMF:DMSO (4:1, v/v), based on the stoichiometry of $Cs_{0.05}(MA_{0.23}FA_{0.77})_{0.95}Pb(Br_{0.23}I_{0.77})_3$. Additives of 2 mol% NH_4SCN and 1.5 mol% NH_4BF_4 were included in the precursor. The solution was spin-coated at 4000 rpm for 40 s, during which 100 µL of CB was dropped onto the wet film 15 s before the end of the spin process. The films were then annealed at 100 °C for 30 min in a nitrogen-filled glovebox. A $PDAI_2$ solution (0.5 mg mL^{-1} in a 1:1 volume ratio of IPA and toluene) was spin-coated onto the perovskite layer at 4000 rpm, followed by thermal annealing at 100 °C for 5 min. Following the surface treatment, a 15 nm-thick C_{60} layer was deposited via thermal evaporation at a rate of 0.1 Å s^{-1}, serving as the electron transport layer (ETL). Subsequently, polyethylenimine ethoxylated (PEIE, 0.2 wt% in methanol) was dynamically spin-coated onto the C_{60} layer.

For opaque devices, a 120 nm-thick Ag electrode was deposited via thermal evaporation. For semi-transparent devices, a 50 nm-thick ITO top electrode was deposited by RF sputtering at room temperature (working pressure: 2 mTorr, power: 50 W, Ar 20 sccm), followed by a 120 nm-thick Ag grid deposited via thermal evaporation.

Fabrication of Si/perovskite tandem solar cells

On top of the commercial Silicon bottom cell, SAM/perovskite/C_{60}/PEIE layers were fabricated using the same process as semitransparent perovskite single-junction solar cells. A 50 nm-thick ITO layer was deposited by a radio frequency sputtering system through the following conditions; deposition rate of 10 nm min^{-1}, working pressure of $2.0x10^{-3}$ mTorr, base pressure under $2.0x10^{-6}$ mTorr, and power of 50 W. A 500 nm-thick Ag layer and a 90 nm-thick LiF layer were deposited by thermal evaporation at a rate of 1.5 Å s^{-1}.

Device characterization

The photocurrent density-voltage (*J–V*) characteristics of single-junction and multi-junction solar cells were measured using a solar simulator (PEC-L11, Pecell Technologies, AAA graded) under 1-sun illumination condition (AM 1.5G), which was calibrated by standard Si cell with quartz filter (91150V, Newport). The *J–V* measurements were conducted with aperture whose size is 0.14 cm^2 for single-junction devices and 0.1875 cm^2 for single-junction and multi-junction tandem devices. The scan rates of *J–V* were 120 and 240 mV s^{-1} for single-junction devices and tandem devices, respectively. The *J–V* scans were conducted in ambient atmosphere at room temperature without any preconditioning such as light soaking. The external quantum efficiency (EQE) spectrum of single-junction devices was measured without light or electrical bias (QUANTX-300, Oriel). The EQE spectrum of perovskite top cell of double-junction tandem devices were measured under an infrared light bias combined with as electrical bias (0.6 V), followed by the measurement of the Si bottom cell under a blue light bias with as electrical bias (1.2 V). The optical properties of the films were measured by UV-vis spectroscopy (Cary5000, Agilent) The crystal phases of films were investigated by X-ray diffraction with Cu Kα radiation (XRD; New D8 advance, Bruker). The top-view and images of films and devices were observed by SEM (SU-70). The surface morphology images were obtained by AFM (Atomic Force Microscope NX-10). Electrochemical Impedance spectroscopy (EIS) was performed in dark conditions using a potentiostat (ZENNIUM, ZAHNER). TPVD measurements were performed using an oscilloscope (MDO3000, Tektronix) with a white-light-emitting lamp (MWWHLP1, Thorlabs) and a 405 nm pulsed laser (iBeam smart 405-S-HP, Toptica) as a light bias and probing light, respectively. PL data was collected by periodically measuring the PL spectrum at room temperature under ambient conditions with continuous 405 nm laser illumination (FluoTime 300, PicoQuant).

Supplementary Figures

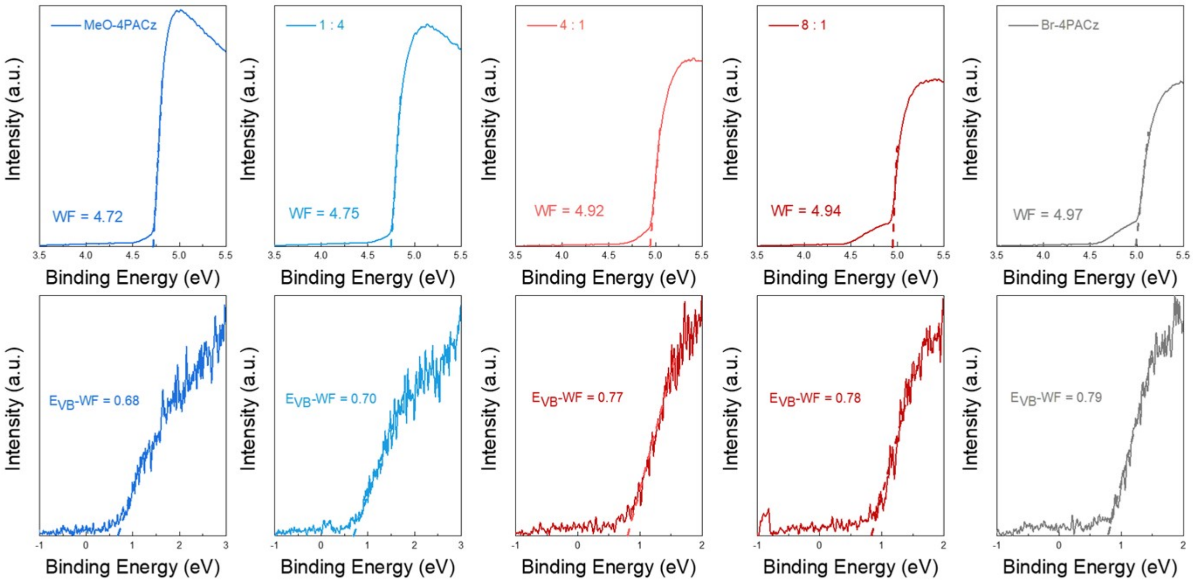

Fig. S1 UPS spectra of SAMs with various Br-4PACz:MeO-4PACz ratios.

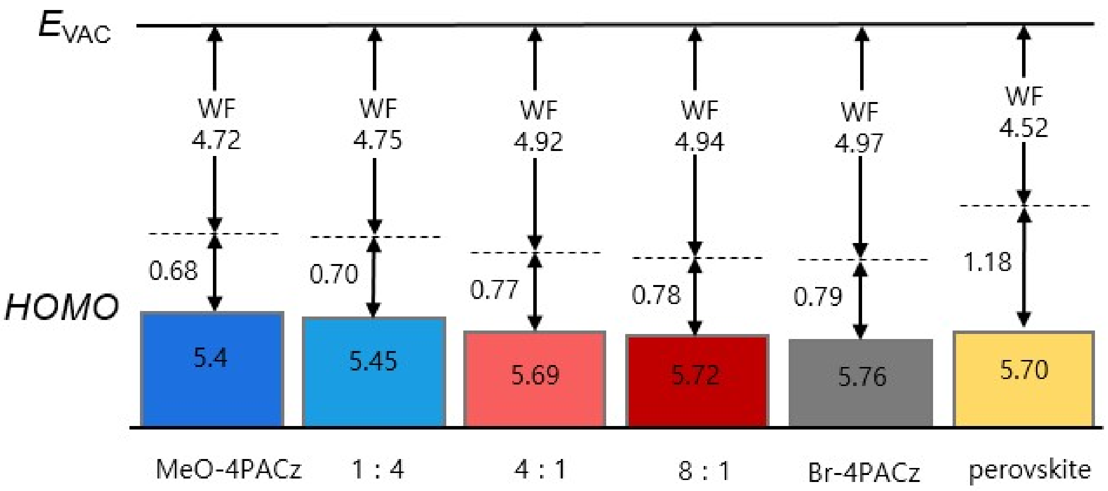

Fig. S2 Energy band diagram of SAMs with various Br-4PACz:MeO-4PACz ratios.

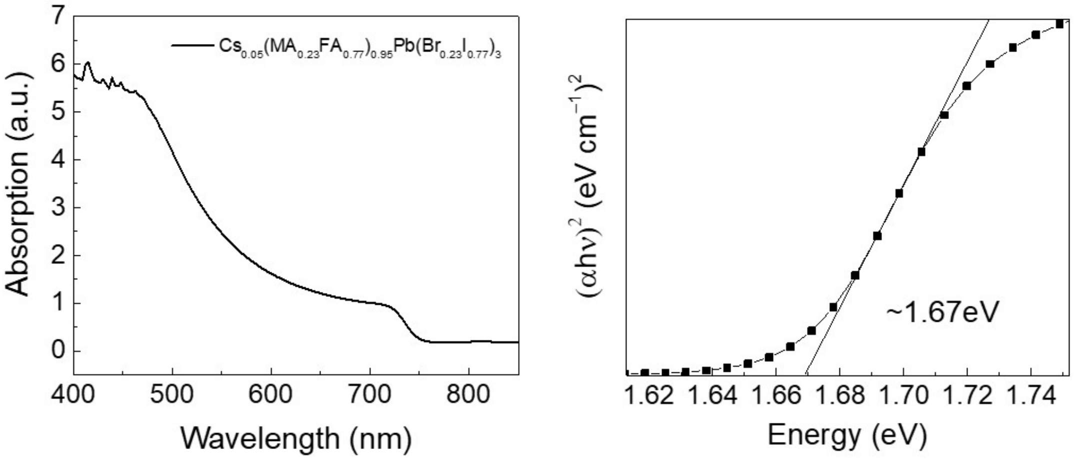

Fig. S3 UV-vis absorption spectra and Tauc plot of the wide-bandgap perovskite film.

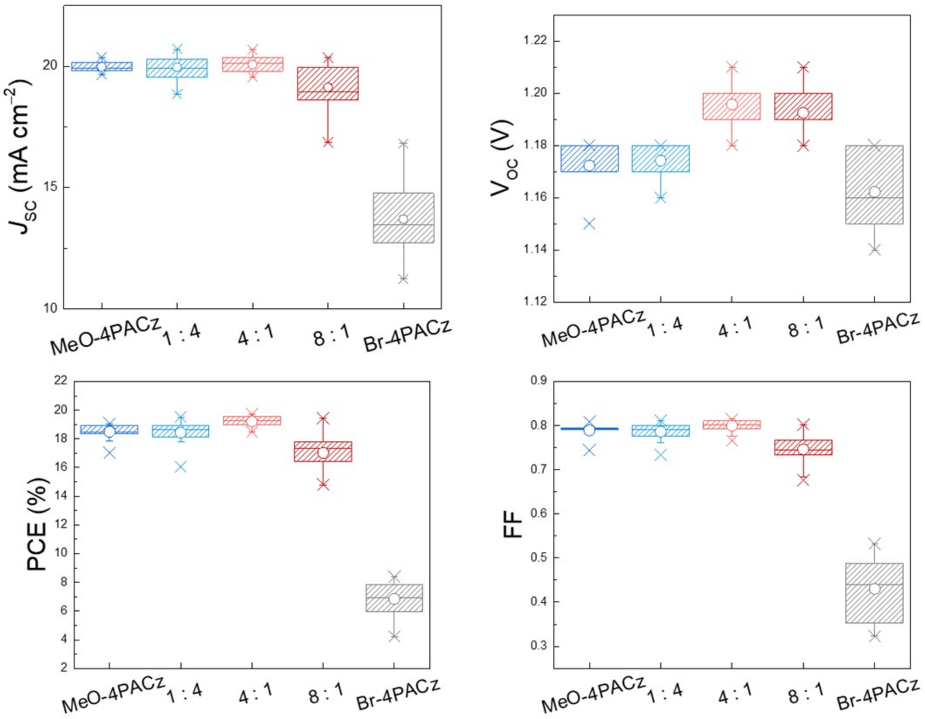

Fig. S4 Statistical photovoltaic parameters of perovskite single-junction solar cells with various Br-4PACz:MeO-4PACz ratios.

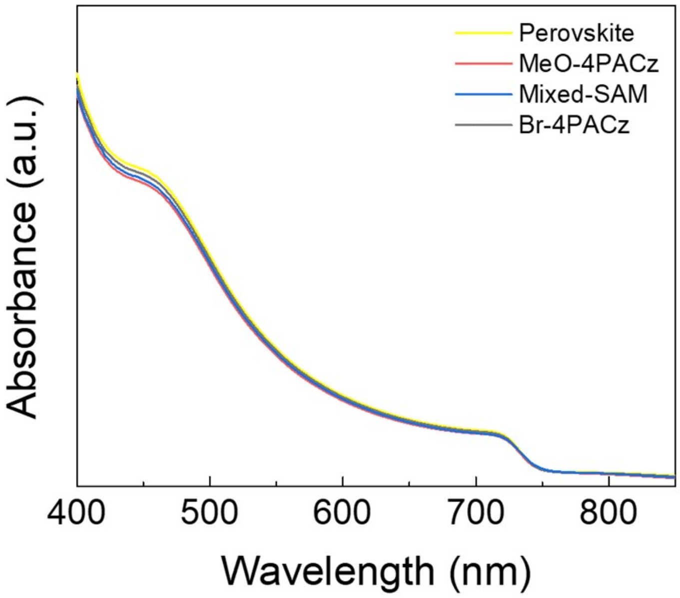

Fig. S5 UV-vis spectra of perovskite film with different SAMs.

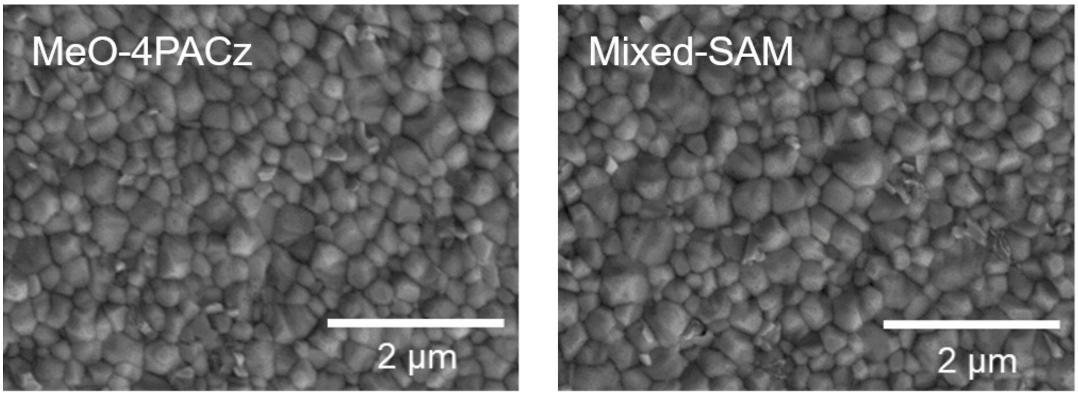

Fig. S6 FE-SEM images of perovskite film with MeO-4PACz and mixed-SAM.

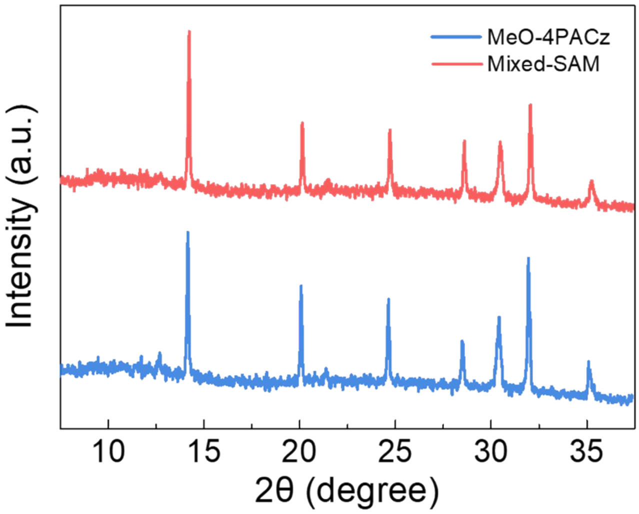

Fig. S7 XRD results of perovskite film with MeO-4PACz and mixed-SAM.

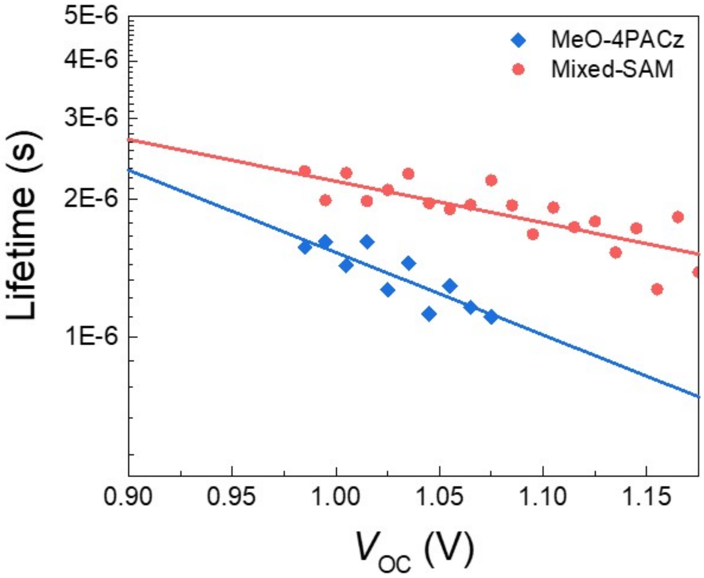

Fig. S8 TPVD curves of the perovskite single-junction solar cells with MeO-4PACz and mixed-SAM.

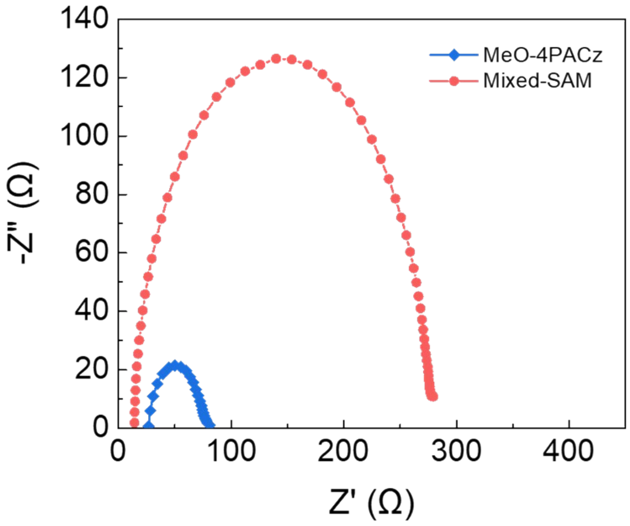

Fig. S9 Nyquist plot of the perovskite single-junction solar cells with MeO-4PACz and mixed-SAM.

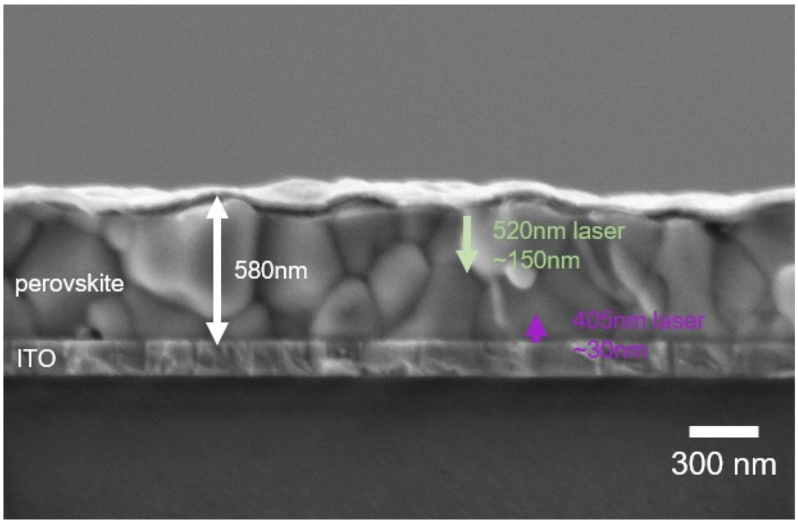

Fig. S10 Cross sectional SEM image depicting the penetration depth depending on the excitation wavelength.

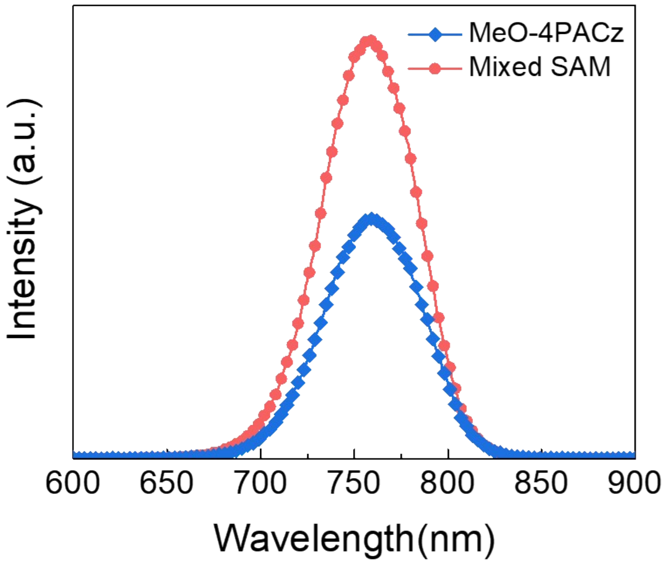

Fig. S11 SS-PL spectra of the ITO/SAMs/perovskite film under 520 nm laser irradiation.

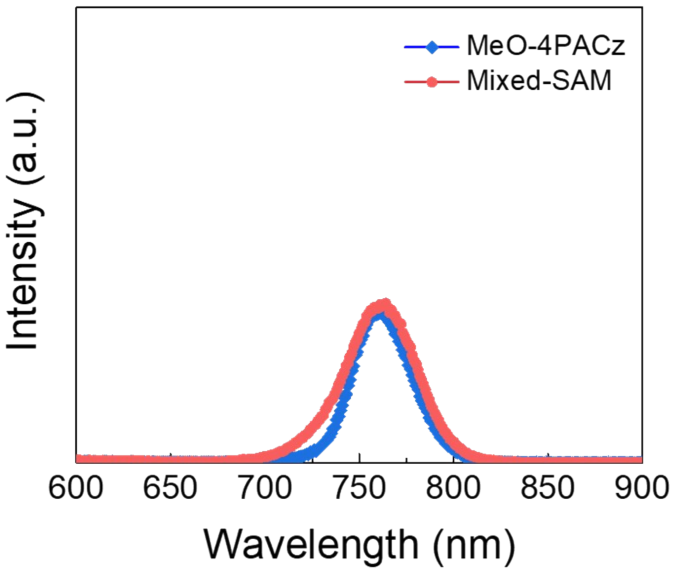

Fig. S12 SS-PL spectra of the ITO/SAMs/perovskite/C_{60} device under 405 nm laser irradiation.

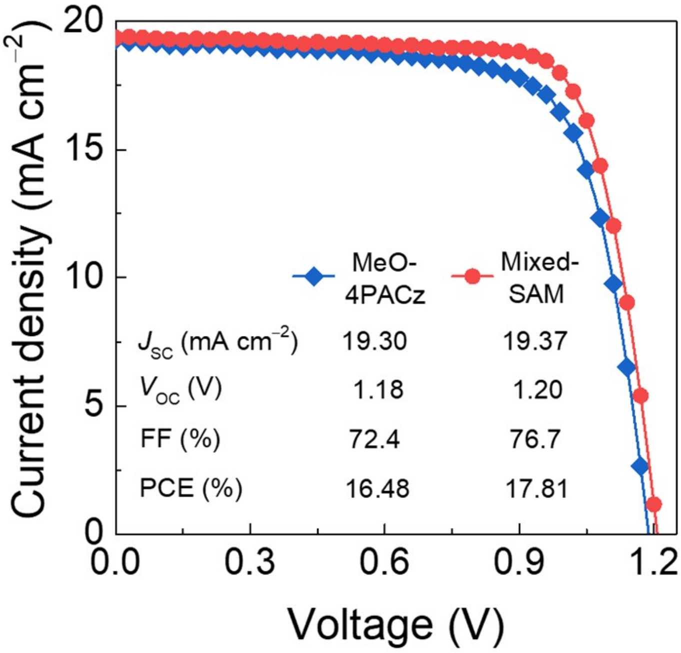

Fig. S13 *J*−*V* curves of the semi-transparent single-junction perovskite solar cells with MeO-4PACz and mixed-SAM.

Table. S1 Photovoltaic and diode parameters of single-junction perovskite solar cells with MeO-4PACz, mixed-SAM and Br-4PACz.

	J_{SC} (mA cm^{-2})	V_{OC} (V)	FF (%)	PCE (%)	R_{sh} (kΩ cm^{-2})	R_S (Ω cm^2)
MeO-4PACz	20.15	1.18	78.71	18.71	36.86	13.38
Mixed-SAM	20.41	1.2	80.54	19.72	46.67	5.49
Br-4PACz	18.74	1.18	55.94	12.37	4.06	635.79